Oxidation of Cu^{II} to Cu^{III}, Free Radical Production, and DNA Cleavage by Hydroxy-salen−Copper Complexes. Isomeric Effects Studied by ESR and Electrochemistry

Eric Lamour,[†] Sylvain Routier,[†] Jean-Luc Bernier,[†] Jean-Pierre Catteau,[†] Christian Bailly,[‡] and Hervé Vezin*[,†]

Contribution from the Laboratoire de Chimie Organique Physique, URA CNRS 351, USTL Bât. C3, 59655 Villeneuve d'Ascq, and INSERM U124 et Laboratoire de Pharmacologie Moléculaire Antitumorale du Centre Oscar Lambret, IRCL, Place de Verdun, 59045 Lille, France

Received June 25, 1998

Abstract: A series of copper complexes of bis(hydroxysalicylidene)ethylenediamine (hydroxy-salens) have been synthesized. The hydroxy group in the *ortho*, *meta*, or *para* position on each salicylidene unit was added to reinforce the stability of the copper complex and to create a hydroquinone system cooperating with the copper redox system to facilitate the spontaneous formation of oxidizing Cu^{III} species. Cyclic voltammetry and ESR spectroscopy in combination with electrochemistry and spin trapping experiments have been used to characterize the structure and the redox state of the hydroxy-salen−copper complexes and to evidence the production of oxygen-based free radicals. A complete set of magnetic values were determined. In addition, we studied the capacity of complexes **3a,b,c** to cleave DNA in the *absence* of activating agents. The *meta* isomer **3b** does not generate oxygen radicals, and as a result it cannot cleave DNA. In sharp contrast, the *para* isomer **3c** and to a lower extent the *ortho* isomer **3a** exhibit nuclease activities in relation to their capacities to produce oxygen radicals. Electrochemistry provides unequivocal evidence for the formation of Cu^{III} species with compounds **3a** and **3c**, but not with **3b**. The nuclease activity correlates well with the ability of the hydroxy-salens to form the oxidizing Cu^{III} species. The redox properties and therefore the DNA cleaving activities of the complexes depend crucially on the position of the OH groups which contribute significantly to stabilize the square planar copper complexes. The present work supports the hypothesis that a hydroquinone system can cooperate with a redox metal system to trigger DNA cleavage. The design of metallo(hydroxy-salens) provides an original route for the development of self-activated chemical nucleases.

Introduction

The trivalent state of copper is generally considered to be an uncommon oxidation state; however, it occurs in reactions relevant to biological processes. A few naturally occurring chelating peptides can decrease sufficiently the oxidation potential of Cu^{III} in order to enable its formation by mild oxidants.[1−5] Low electrode potential ($E°$) values ranging from 0.45 to 1.05 V/SHE have been measured for various peptides[6−8] containing deprotonated nitrogens as strong σ donors in order to stabilize the higher oxidation state of copper.[9−11] Low values of the Cu^{III}/Cu^{II} electrode potential were also determined for macrocyclic complexes such as cyclo[G-βA-G-βA]−Cu ($E° = 0.48$ V in aqueous solution).[12] High oxidation state transition complexes represent useful models of redox enzymes such as galactose oxidase[13,14] and may serve in nucleic acid chemistry as oxidative DNA damaging agents. With this idea in mind, we designed a strategy to construct a new chemical nuclease which can generate oxidizing Cu^{III} species to trigger DNA cleavage.

A number of copper complexes capable of inducing double-stranded DNA lesions have already been developed.[15−17] Phenanthroline−Cu^{II} and a few related copper complexes have

* To whom correspondence should be addressed.

[†] CNRS.

[‡] INSERM.

(1) Margerum, D. W.; Scheper, W. M.; McDonald, M. R.; Fredericks, F. C.; Wang, L.; Lee, H. D. In *Bioorganic Chemistry of Copper*; Karlin, K. D., Tyeklar, Z., Eds.; Chapman & Hall: New York, 1993; p 213.

(2) Margerum, D. W. In *Oxidases and related Redox-systems*; King, T. E., Mason, H. S., Morrison, M., Eds.; Pergamon Press: Oxford, 1982; p 193.

(3) Kou, F.; Zhu, S.; Lin, H.; Ma, K.; Chu, Y. *Polyhedron* **1997**, *16*, 741.

(4) Margerum, D. W.; Wang, L.; Scheper, W. M.; Wang, L.; Lee, H. D. *J. Inorg. Biochem*. **1991**, *43*, 211.

(5) McDonald, M. R.; Scheper, W. M.; Lee, H. D.; Margerum, D. W. *Inorg. Chem*. **1995**, 34, 229.

(6) Bossu, F. P.; Chellappa, K. L.; Dale, W.; Margerum, D. W. *J. Am. Chem. Soc*. **1977**, *99*, 2195.

(7) Ruiz, R.; Surville-Barland, C.; Ankanloo, A.; Anxolabehere-Mallart, E.; Journaux, Y.; Cano, J.; Carmen Muñoz, M. *J. Chem. Soc., Dalton Trans*. **1997**, 745.

(8) Margerum, D. W.; Chellappa, K. L.; Bossu, F. P.; Burce, G. L. *J. Am. Chem. Soc*. **1975**, *97*, 6894.

(9) Margerum, D. W.; Owens, G. D. In *Metal Ions in Biological Systems*; Sigel, H., Eds.; Marcel Dekker: New York, 1981; p 75.

(10) Youngblood, M. P.; Margerum, D. W. *Inorg. Chem*. **1980**, *19*, 3068.

(11) Bossu, F. P.; Chellappa, K. L.; Margerum, D. W. *J. Am. Chem. Soc*. **1997**, *16*, 2195.

(12) Rybka, J. S.; Margerum, D. W. *Inorg. Chem*. **1981**, *20*, 1453.

(13) Ito, N.; Phillips, S. E. V.; Stevens, L.; Ogel, Z. B.; McPherson, M. S.; Yadav, K. D. S.; Knowles, P. F. *Nature* **1991**, *350*, 87.

(14) Sokolowski, A.; Müller, J.; Weyhermüller, T.; Schnepf, R.; Hildebrandt, P.; Hildenbrand, K; Bothe, E.; Wieghardt, K. *J. Am. Chem. Soc*. **1997**, *119*, 8889.

(15) Huber, P. W. *FASEB J*. **1994**, *7*, 1367−1375.

(16) Pratviel, G.; Bernadou, J.; Meunier, B. *Angew. Chem., Int. Ed. Engl*. **1995**, *34*, 746−769.

(17) Burrows, C. J.; Muller, J. G. *Chem. Rev*. **1998**, *98*, 1109.

10.1021/ja982221z CCC: $18.00
Published on Web 02/23/1999

been extensively exploited for the study of nucleic acid structure and function as well as to investigate drug and protein binding.[18,19] However, in most cases, if not all, the cleavage reaction must be initiated by a reducing agent such as dithiothreitol or mercaptopropionic acid. The DNA cleavage reaction is oxygen-dependent and mediated by reactive oxygen species produced concomitantly with the reduction of Cu^{II} to Cu^{I}. For example, in a typical DNA cleavage experiment, the reaction of Cu^{II} with the reducing agent generates Cu^{I} which then can react with molecular oxygen and/or hydrogen peroxide to produce hydroxyl radicals responsible for DNA breakage. Alternatively, a transient Cu^{II}−oxo intermediate may form.[18,19] It would be of interest to find a self-activated system that would not require reductive activation to generate free radicals and to exert DNA cleavage.

For the past few years our interest has focused on the synthesis of simple, peptidic and nonpeptidic molecules that mimic structural and/or functional aspects of nucleases.[20−25] Our approach exploits the potential of metal complexes of *N*,*N*′-bis(salicylidene)ethylenediamine compounds, usually referred to as metallosalens, which have been used for a long time as catalysts for selective epoxidation of olefins and oxidation of hydrocarbons.[26,27] Salens complexed with various metals (Cu^{II} but also Ni^{II}, Co^{II}, and Mn^{III}) can be used as probes for the cleavage of DNA or RNA.[17,28−33] In a recent study, we showed that salen−Cu complexes can efficiently induce nonspecific DNA damages upon activation with mercaptopropionic acid.[20] Here we report a new type of salen−Cu complex which can give spontaneously the oxidant species Cu^{III} and cleave DNA without an activating agent. This is a new copper-containing self-activated chemical nuclease.[34−36] Only a few nucleases of this type have been reported so far. A variety of methods including ESR and cyclic voltammetry have been employed to characterize the structure of the complexes and their redox state and the production of free radicals and their DNA cleaving activities.

To obtain copper complexes with a low Cu^{III}/Cu^{II} electrode potential, we incorporated a hydroquinone system on the *N*,*N*′-bis(salicylidene)ethylenediamine−copper complex (Scheme 1). We reasoned that the addition of hydroxyl groups in the *ortho*, *meta*, or *para* position on the aromatic ring of the salen moiety would activate the nuclease activity of the copper complexes. On one hand, the newly introduced OH groups should increase the electronic density on the metal by their σ donor effects and lower the Cu^{II}/Cu^{III} electrode potential $E°$. On the other hand, the presence of a hydroquinone may alter the redox properties of the molecule, favoring the formation of an equilibrium in electron transfer through the complex, leading to a semiquinone radical.

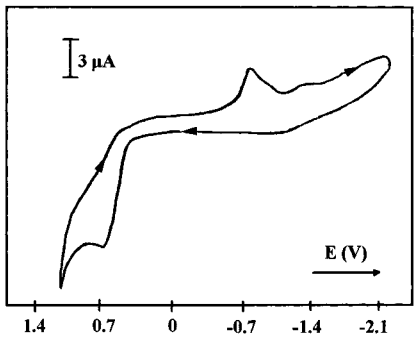

Figure 1. Cyclic voltammogram for the *ortho* ligand **2a** in DMSO containing 0.1 N tetraethylammonium perchlorate. A similar curve was obtained with the *para* analogue **2c**.

Scheme 1

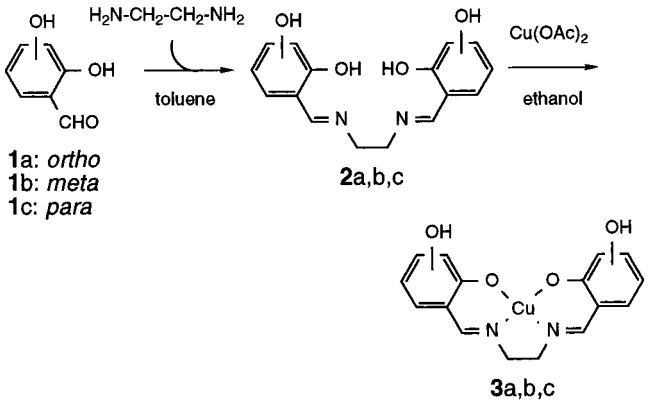

The electrochemical and spectroscopic studies reported here reveal that, depending on the positions of the hydroxyl groups, the redox and structural properties of the copper complexes differ significantly. The *para* isomer **3c** and to a lower extent the *ortho* isomer **3a**, which can form Cu^{III} species, can spontaneously cleave DNA whereas neither the *meta* isomer **3b** nor the non-hydroxylated derivative **3d** have any effect.

Results

Cyclic Voltammetry. For the *ortho* (**2a**) and *para* (**2c**) ligands, the strong oxidation wave (E_{pa} = +0.56 V/SCE at 50 mV s^{-1}) was attributed to a two-electron oxidation of the hydroquinone moiety. No reversible or quasi-reversible oxidation was observed for any of the ligands. Cathodic peaks were detected at −0.74 V after oxidation (Figure 1). No significant oxidation or reduction wave was detected with the *meta* ligand (**2b**).

The cyclic voltammogram of **3a** is shown in Figure 2 as a typical example of the reduction and subsequent oxidation of the hydroxy-salen complexes. A similar curve was obtained with **3c**. Starting from zero potential, a quasi-reversible reduction

(18) Sigman, D. S.; Chen, C.-H. B. *Annu. Rev. Biochem.* **1990**, *59*, 207−236.
(19) Sigman, D. S.; Mazumder, A.; Perrin, D. M. *Chem. Rev.* **1993**, *93*, 2295−2316.
(20) Routier, S.; Bernier, J. L.; Waring, M. J.; Colson, P.; Houssier, C.; Bailly, C. *J. Org. Chem.* **1996**, *61*, 2326.
(21) Routier, S.; Bernier, J. L.; Catteau, J. P.; Bailly, C. *Bioorg. Med. Chem. Lett.* **1997**, *1*, 63.
(22) Routier, S.; Cotelle, N.; Catteau, J. P.; Bernier, J. L.; Waring, M. J.; Riou, J. F.; Bailly, C. *Bioorg. Med. Chem.* **1996**, 4, 1185.
(23) Routier, S.; Bernier, J. L.; Catteau, J. P.; Colson, P.; Houssier, C.; Rivalle, C.; Bisagni, E.; Bailly, C. *Bioconjugate Chem.* **1997**, *6*, 7789.
(24) Routier, S.; Bernier, J. L.; Catteau, J. P.; Bailly, C. *Bioorg. Med. Chem. Lett.* **1997,** *13*, 1729.
(25) Routier, S.; Joanny, V.; Zaparucha, A.; Vezin, H.; Catteau, J. P.; Bernier, J. L.; Bailly, C. *J. Chem. Soc., Perkin Trans 2* **1998**, *4*, 863.
(26) Breslow, R.; Zhang, X.; Xu, R.; Maletic, M.; Merger, R. *J. Am. Chem. Soc.* **1996**, *118*, 11678.
(27) Adam, W.; Fell, R. T.; Stegmann, V. R.; Saha-Möller, C. R. *J. Am. Chem. Soc.* **1998**, *120*, 708.
(28) Muller, J. G.; Chen, X.; Dadiz, A. C.; Rokita, S. E.; Burrows, C. J. *J. Am. Chem. Soc.* **1992**, *114*, 6407.
(29) Gravert, D. J.; Griffin, J. H. *J. Org. Chem.* **1993**, *58*, 820.
(30) Muller, J. G., Paikoff, S. J., Rokita, S. E., Burrows, C. J. *J. Inorg. Biochem.* **1994**, *54*, 199.
(31) Gravert, D. J.; Griffin, J. H. *Inorg. Chem.* **1996**, 35, 4837.
(32) Burrows, C. J.; Rokita, S. E. *Acc. Chem. Res.* **1994**, *27*, 295.
(33) Bhattacharya, S.; Mandal, S. S. *J. Chem. Soc., Chem. Commun.* **1995**, *24*, 2489.
(34) Lytollis, W.; Scannell, R. T.; An, H.; Murty, V. S.; Reddy, K. S.; Barr, J. R.; Hecht, S. M. *J. Am. Chem. Soc.* **1995**, *117*, 12683.
(35) Singh, U. S.; Scannell, R. T.; An, H.; Carter, B. J.; Hecht, S. M. *J. Am. Chem. Soc.* **1995**, *117*, 12691.
(36) Borah, S.; Melvin, M. S.; Lindquist, N.; Manderville, R. A. *J. Am. Chem. Soc.* **1998**, *120*, 4557.

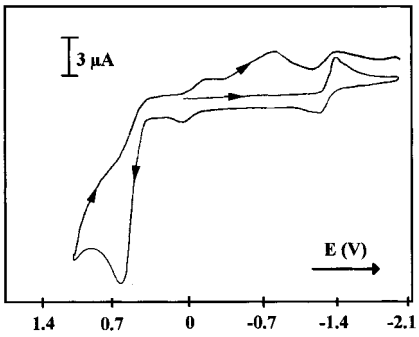

Figure 2. Cyclic voltammogram for the *ortho* copper complex **3a** in DMSO containing 0.1 N tetraethylammonium perchlorate. A similar curve was obtained with the *para* analogue **3c**.

and subsequent oxidation ($\Delta E = 130$ mV) assigned to the one-electron transfer $Cu^{I} \rightarrow Cu^{II}$ was observed at $E_{1/2} = -1.33$ V/SCE. Another quasi-reversible wave ($\Delta E = 200$ mV) observed at $E_{1/2} = -0.100$ V/SCE was assigned to oxidation of $Cu^{II} \rightarrow Cu^{III}$. The strong oxidation wave at +0.55 mV and reduction wave at −0.82 V are representative of the oxido-reduction of the quinone moiety as mentioned above (Figure 1). Similar experiments were carried out with the non-hydroxylated salen−Cu^{II} complex. In this case, only one quasi-reversible oxido-reduction wave was observed at −1.0 V. It is assigned to the one-electron transfer $Cu^{II} \rightarrow Cu^{I}$ (Figure 2). The cyclic voltammogram of complex **3b** did not show any oxido-reduction wave.

Electron Spin Resonance. Figure 3 displays the ESR spectra of compounds **3a,b,c** obtained in liquid nitrogen (77 K, Figure 3a) and at room temperature (20 °C, Figure 3b). The three equally spaced ESR peaks, shown in Figure 3a and observed at low magnetic field, are related to the hyperfine coupling of Cu^{II}. The parallel components $g_{||}$ and $A_{||}$ were determined from the spectrum at low temperature. The perpendicular region is more difficult to interpret due to the absence of superhyperfine structure in the $g_{||}$ region. Therefore, the perpendicular components cannot be precisely determined. However, the ESR spectrum in free tumbling motion at room temperature (Figure 3b,c) enabled us to determine the average value of the isotropic components g_o and A_o from which the perpendicular components $g_\perp$ and $A_\perp$ can be calculated using the relationships $g_o = (g_{||} + 2g_\perp)/3$ and $A_o = (A_{||} + 2A_\perp)/3$. The ESR parameters of the hydroxysalen−Cu^{II} complexes are reported in Table 1. Figure 3c displays the ESR signal of compound **3c** obtained after addition of a small amount of NaOH (1 M) in order to activate the hydroquinonic system. In this case, the Cu^{II} ESR signal is strongly decreased (up to 60%). The same phenomenon was observed with **3a** but not with **3b**, which cannot form a semiquinone.

ESR spectra of Cu^{II} ions can be described by the spin Hamiltonian[37]

$$\mathbf{H}_{Cu} = \mu_B \vec{\mathbf{H}} \vec{\mathbf{g}}_{Cu} \cdot \vec{\mathbf{S}}_{Cu} + \vec{\mathbf{S}}_{Cu} \cdot \vec{\mathbf{A}}_{Cu} \cdot \vec{\mathbf{I}}_{Cu} + \sum_{Ni} \vec{\mathbf{S}}_{Cu} \cdot \vec{\mathbf{A}}_{Ni} \cdot \vec{\mathbf{I}}_{Ni}$$

where $\vec{\mathbf{S}}_{Cu} = 1/2$ and $\vec{\mathbf{I}}_{Cu} = 3/2$ are the electronic and nuclear spins of copper, respectively. The two hyperfine tensors $\vec{\mathbf{g}}_{Cu}$ and $\vec{\mathbf{A}}_{Cu}$ of copper expressed the coupling strength of its electronic spin with the applied magnetic field and nuclear magnetic moment associated with $\vec{\mathbf{I}}_{Cu}$. The last term refers to the superhyperfine interaction resulting from the coupling of copper electronic spin with nuclear spin $\vec{\mathbf{I}}_{Ni}$ of the nitrogen ligand. Figure 4a diplays the experimental second-derivative spectrum of 100 G expansion of the $m_I = +3/2$ line of the isotropic spectrum of Figure 3b. The spectrum exhibits 10 lines which can be attributed to the superhyperfine interactions of the two equivalent nitrogen nuclei of the complex with the nuclear spin of isotopes ^{63}Cu and ^{65}Cu with identical intensities of 1:2:3:2:1. The simulated spectrum (Figure 4b) was determined using a hyperfine coupling splitting constant of 14.25 G for both nitrogens. The result gives a good fit with the experimental spectrum.

The *g* values and hyperfine splitting constants are related to the matrixes **g** and **A**, respectively. From the experimental data, we measured for all complexes the $g_{||}$ values which are in agreement with the relation $g_{zz} > g_{xx,yy}$, indicating that we are in the presence of a $d_{x^2-y^2}$ ground state. This arrangement is

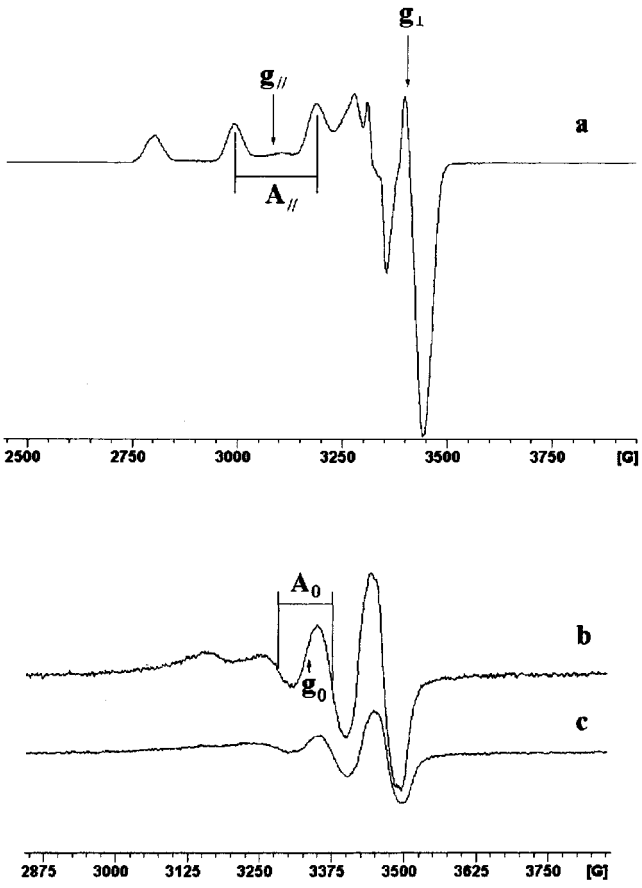

Figure 3. Experimental X-band ESR spectra of the *para* copper complex **3c** at 2 mM in DMSO (a) at liquid nitrogen temperature (77 K), (b) at room temperature, and (c) in the presence of NaOH. The receiver gain was 1.25×10^4. Magnetic parameters are reported in Table 1.

Table 1. ESR Parameters of the Salen−Cu Complexes

	g values			*A* values (^{63}Cu, $\times 10^4$ cm^{-1})				
	g_{iso}	$g_{||}$	$g_\perp$	A_{iso}	$A_{||}$	$A_\perp$	α^2	k
Without NaOH								
ortho (**3a**)	2.100	2.207	2.046	−83.5	−181.1	−34.73	0.69	0.33
meta (**3b**)	2.098	2.207	2.043	−85.6	−181.1	−37.88	0.68	0.33
para (**3c**)	2.098	2.207	2.043	−86.7	−182.4	−38.86	0.69	0.34
3d	2.050	2.210	1.970	−83.0	−178.6	−35.20	0.72	0.28
With NaOH								
ortho (**3a**)	2.094	2.230	2.026	−86.5	−185.2	−37.20	0.73	0.33
meta (**3b**)	2.092	2.210	2.033	−88.3	−183.3	−40.90	0.69	0.33
para (**3c**)	2.095	2.220	2.033	−88.4	−191.7	−36.70	0.74	0.34

(37) Abragam, A.; Bleaney, B. *Electron Paramagnetic Resonance of Transition Ions;* Clarendon Press: Oxford, U.K., 1970.

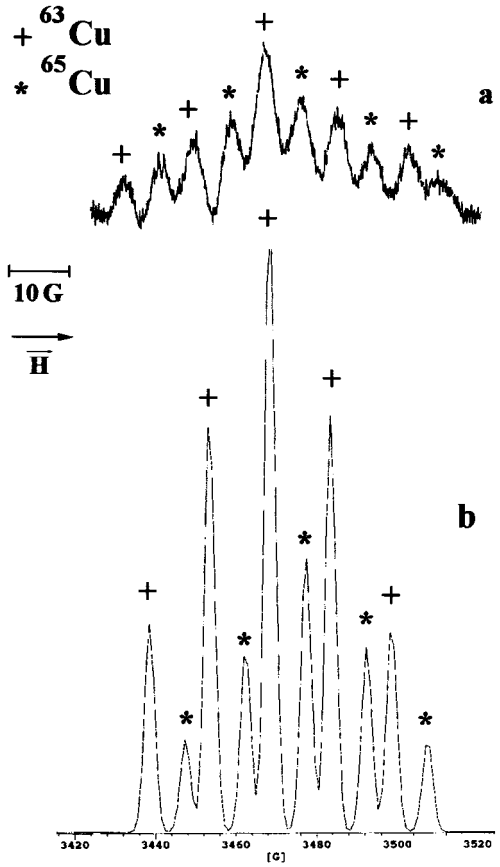

Figure 4. Experimental (a) and simulated (b) ESR spectra of the copper complex **3c** in DMSO solution at room temperature. The experimental spectrum (a) corresponds to a 100 G expansion of the second harmonic 90° out of phase $m_I = +3/2$ copper component. The theoretical spectrum (b) was simulated considering two equivalent nitrogen nuclei coupled to ^{63}Cu and ^{65}Cu nuclear spin at relative natural isotopic abundance. $A^{N}_{iso} = -0.0013$ cm^{-1}.

characteristic of a square-planar, a square base pyramidal, or an octahedral geometry.[38,39] From the equation describing the molecular antibonding orbitals, which are related to the Hamiltonian spin parameters, we can write the magnetic parameters as follows:

$$A_{\parallel} = P\left(-k - \frac{4\alpha^2}{7} + (g_{\parallel} - 2.0023) + \frac{3(g_{\parallel} - 2.0023)}{7}\right)$$

$$A_{\perp} = P\left(-k + \frac{2\alpha^2}{7} + \frac{11(g_{\perp} - 2.0023)}{14}\right)$$

We used these two equations together with the g and A values previously calculated to measure the extent of ionic bonding α^2 and the extent contact term k.[40] The α^2 factor is related to the unpaired electron density on the d-orbital of Cu^{II}. This factor results from the dipole−dipole interaction between magnetic moments associated with the spin of the electron and the nucleus and is closely related to the $A_{\parallel}$ value.

The α^2 values for the complexes **3a,b,c** are lower than that calculated for the non-hydroxylated complex (Table 1). This can be attributed to an increase of covalency due to the donor effect of the hydroxyl groups. It is important to note that when the hydroquinonic system is activated by addition of small amounts of NaOH, we observed a significant increase of α^2 for **3a** and **3c** complexes, suggesting an increase of ionic copper ligand bonding most likely due to the formation of a semiquinone radical. In the case of the **3b** complex, the semiquinone radical cannot form, and as a result, the α^2 value remains almost unchanged. The k value arises from the Fermi contact interaction. Its origin comes from the nonvanishing probability of finding the unpaired electron at the nucleus site.[40] The k values obtained with compounds **3a,b,c** in the presence or absence of NaOH (i.e., independently of the semiquinonic system) are higher than that obtained with the non-hydroxylated complex. The k value for the non-hydroxylated compound is consistent with a tetrahedral distortion of the symmetry around the metal ion explained by the reduction of the anisotropic hyperfine term.

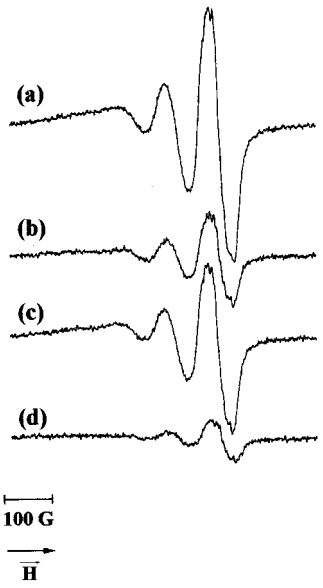

Figure 5. Experimental ESR spectra in combination with electrochemistry of compound **3c** at 2 mM in DMSO and at room temperature: (a) reference spectrum, (b) −1.4 V, (c) 0 V, and (d) +0.5 V. The receiver gain was 1.25×10^4.

Coupling to Electrochemistry. To investigate further the redox state of the copper complexes, we performed a series of experiments by combining electrochemistry with ESR measurements. The ESR signals were measured under potential at the characteristic values found by cyclic voltammetry. Figure 5 shows the results obtained with **3c** using DMSO as a solvent. The reference signal in Figure 5a corresponds to the complex in the absence of current. Imposed potentials of −1.4, −0.01, and +0.5 V gave the signals represented in parts b−d, respectively, of Figure 5. At the lowest potential (−1.4 V) a strong decrease (∼60%) of the copper(II) ESR signal is observed, resulting from a reduction of Cu^{II} to Cu^{I}. When the potential is brought back to a value near 0 V, the typical Cu^{II} signal is partially restored (Figure 5c). The uncomplete restoration of the signal may be due to the fact that at ∼0 V, we are approaching the potential of Cu^{III} which is an ESR silent species. For a potential of +0.5 V, a strong drop of the ESR signal is observed (>80%), suggesting an almost complete oxidation of Cu^{II} to Cu^{III} (Figure 5d). At this stage, a very weak and unstable signal of 20 G sweep width was detected. It may be attributable to the formation of a semihydroquinone radical (Figure S4 in the Supporting Information).

Spin trapping experiments were performed to detect reactive oxygen species produced upon variation of the redox state of copper. These experiments were also performed in combination with electrochemistry. Both DMSO and ethanol were used as

(38) Hathaway, B. J.; Tomlinson, A. A. G. *Coord. Chem. Rev.* **1970**, *5*, 1.
(39) Hathaway, B. J.; Billing, D. E. *Coord. Chem. Rev.* **1970**, *5*, 143.
(40) Maki, A. H.; McGarvey, B. R. J. *Chem. Phys.* **1958**, *29*, 31.

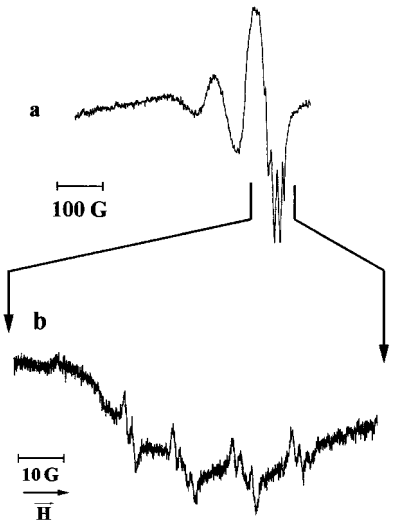

Figure 6. Experimental X-band ESR spectra of compound **3c** at 2 mM in DMSO and at room temperature in the presence of 3.2 mM DMPO (a). Spectrum (b) corresponds to a 100 G expansion of the $m_I = +3/2$ copper component of the DMPO−OOH spin adduct. The hyperfine splitting constants are $a_N = 14.35$, $a_H = 12.75$, and $a_{H\gamma} = 1.5$ G.

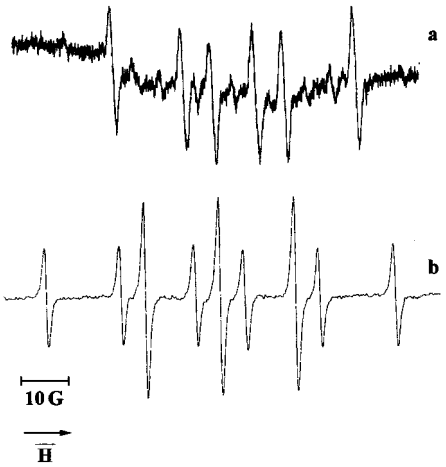

Figure 7. Experimental ESR spectra of (a) the DMPO−CH_3 spin adduct ($a_N = 14.7$ and $a_H = 21$ G) and (b) the DMPO−H spin adduct ($a_N = 15.75$ and $a_H = 20.37$ G). The ESR spectra were obtained in combination with electrochemistry using a 2 mM solution of compound **3c** at room temperature in the presence of 3.2 mM DMPO. The applied potentials were (a) −1.4 V and (b) +0.5 V.

solvents, and 5,5′-dimethylpyrroline *N*-oxide (DMPO) provided the spin trapping agent. Figure 6 displays the spectra recorded in a pure DMSO solution. A typical Cu^{II} ESR signal with four lines superimposed on the $m_I = +3/2$ line was observed (Figure 6a). A closer view of the spectrum (100 G sweep width in Figure 6b) revealed the presence of an ESR signal corresponding to the DMPO adduct of the superoxide anion radical $O_2^{\bullet-}$ produced by compounds **3a** and **3c**. The hyperfine splitting constants $a_N = 14.35$, $a_H = 12.75$, and $a_{H\gamma} = 1.5$ G are characteristic of a DMPO−OOH spin adduct (simulated spectrum in Figure S1 in the Supporting Information). Moreover, there is a modification of the spectrum line shape, indicating the presence of overlapped Cu^{II} species.

With the coupling of electrochemistry (Figure 7), two different spin adducts were detected depending on the reductive (−1.4 V) or oxidative (+0.5 V) conditions. When a potential of −1.4 V was applied to the solution, the spin adduct DMPO−CH_3 was detected (ESR parameters for hyperfine splitting constants $a_N = 14.7$ and $a_H = 21$ G in Figure 7a, simulated spectrum in Figure S2 in the Supporting Information). The DMPO−CH_3 spin adduct is a well-known signature for the production of hydroxyl radicals which decompose in DMSO.[41,42] At a higher potential (+0.5 V), a drastic change in trapped species occurs. Indeed, the spectrum shown in Figure 7b can be attributed to the spin adduct DMPO−H with hyperfine splitting constants $a_N = 15.75$ and $a_H = 20.37$ G (simulated spectrum in Figure S3 in the Supporting Information). This spectrum is consistent with the formation of a semiquinone radical by a homolytic cleavage of the OH groups, producing $H^{\bullet}$ radicals trapped by DMPO.

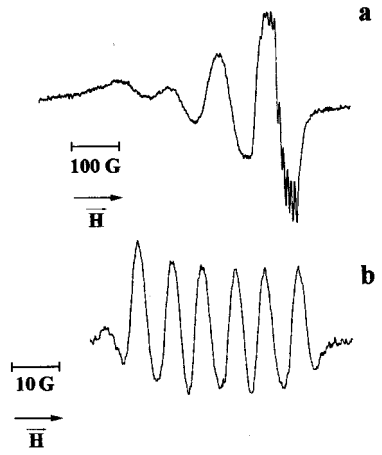

Figure 8. (a) ESR spectrum of compound **3c** in ethanol at room temperature. A 100 G expansion of the second derivative of the $m_I = +3/2$ copper component is shown in (b). DMPO−copper complex adduct with hyperfine splitting constants $a_N = 13$ G and $a_{H\beta} = 7.7$ G.

The ESR spectra obtained with compounds **3a** and **3c** recorded in ethanol show a six-line superimposed spectrum on the $m_I = 3/2$ line of the Cu^{II} species (Figure 8a). The second-derivative 100 G expansion spectrum gave $a_N = 13$ G and $a_{H\beta} = 7.7$ G (Figure 8b). The relative magnitude of the *A* value with $a_N > a_{H\beta}$ indicates that an oxygen-centered radical has been trapped. We can speculate the formation of a $Cu^{II}-O_2$ complex which has one unpaired electron and that this species is trapped to yield the spin adduct shown in Figure 8. Magnetic nuclei more than three bond lengths away from the nitroxide usually do not cause resolvable splitting. Therefore, hyperfine splitting due to the copper nucleus is not expected.

DNA Cleavage. The ESR data reported above revealed clear differences between the hydroxy-salen derivatives depending on the presence and the position of the OH groups. Accordingly, the DNA cleaving capacities of the compounds differ substantially. DNA cleavage was analyzed by monitoring the conversion of supercoiled plasmid DNA (form I) to the nicked circular molecules (form II) and linear DNA (form III). The experiments were performed in the absence of an activating agent (no MPA) in order to satisfy the imposed conditions. It can be seen in Figure 9 that neither the non-hydroxylated compound nor the *meta* derivative **3b** causes any detectable cleavage of nucleic acid. The extent of nicked DNA is identical to that of the control with no ligand present in it. In sharp contrast, the *ortho* (**3a**) and *para* (**3c**) derivatives significantly promote DNA cleavage in the absence of activator. **3c** is more effective than **3a**. Under the conditions specified in the caption of Figure 9a, compound **3c** causes substantial DNA cleavages with a nearly complete

(41) Britigan, B. E.; Rosen, G. M.; Chai, Y.; Cohen, M. S. *J. Biol. Chem.* **1986**, *261*, 4426.
(42) Finkelstein, E.; Rosen, G. M.; Rauckman, E. J. *Arch. Biochem. Biophys.* **1980**, *200*, 1.

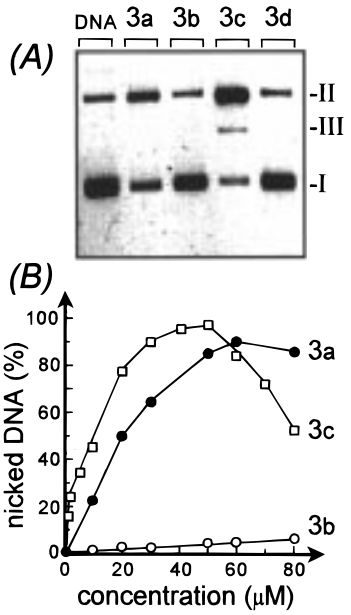

Figure 9. (A) Cleavage of closed circular DNA. Supercoiled DNA (0.6 μg) was incubated at 37 °C for 2 h with the copper complexes **3a,b,c** at 50 μM. Forms I, II, and III refer to the supercoiled, nicked, and linear DNA forms, respectively. (B) Comparison of the cleavage efficiency of the *ortho*, *meta*, and *para* complexes. The plots show the formation of nicked DNA (form II) as a function of the ligand concentration.

conversion of form I to the nicked form II and the appearance of linearized DNA molecules (form III; excess single-strand breaks enhance the probability of double-strand scissions). The dose-dependent curves in Figure 9b corroborate these observations. No cleavage can be detected with **3a** and its non-hydroxylated counterpart, even at a concentration as high as 1 mM. **3c** is the most efficient nuclease in the series. It can convert supercoiled DNA into nicked DNA at low concentrations in the absence of MPA. Parenthetically, we noted that all four ligands induce roughly similar extents of DNA cleavage in the presence of 100 μM mercaptopropionic acid (MPA) as a reducing agent ($Cu^{II} \rightarrow Cu^{I}$ reductive pathway, data not shown). The biochemical results are in perfect agreement with the voltammetry and ESR data.

Discussion

The *para* isomer **3c** exhibits a remarkable nuclease activity. The cleavage of DNA arises most likely from the attack by reduced oxygen species which can be identified by spin trapping experiments (Figures 6 and 7). The ESR and voltammetry data with **3c** (and **3a** as well) are consistent with the reaction pathway indicated in Figure 10. Two main chemical routes can be envisaged for the reaction of the Cu^{II}−hydroquinone complex with molecular oxygen. The first pathway involves direct activation of the quinone system. Indeed, we cannot exclude the possibility that the production of $O_2^{\bullet -}$ radicals results from the activation of the hydroquinone into a semiquinone. In this case, the Cu^{II}−quinone$^{\bullet}$ species initially formed would then transform into the corresponding Cu^{III}−quinone^{-} form.[43] The second pathway is more likely to occur and involves the formation of a dioxygen−Cu^{II} complex (as judged from the typical ESR spectrum in Figure 8) in equilibrium with a Cu^{III}−O_2^{-} intermediate preceding the formation of the Cu^{III}−hydroquinone species. Such metal−dioxygen complexes have been described with cobalt complexes.[43,44] Additional experiments performed under oxygenation conditions also agree with the formation of a dioxygen−metal complex. Indeed, under oxygen we detected a strong ESR signal characteristic of the DMPO−OOH adduct when the ligand was dissolved in DMSO, and a dioxygen−metal complex spin adduct was detected when the ligand was dissolved in ethanol. At the same time, the signal of the Cu^{II} complex disappeared almost completely (spectra not shown). All the data concur that a superoxo−Cu^{III} intermediate does form prior to the production of superoxide anions. The voltammogram of **3a,c** attests that both complexes can form Cu^{III} species at low potential values (Figure 2). The effect is directly attributable to the presence on the aromatic ring of two hydroxyl groups in the *ortho* or *para* positions. The formation of a Cu^{III} intermediate is new but not entirely surprising since it is known that the Cu^{II}/Cu^{III} potential of copper complexes is strongly reduced near 0 V versus a standard calomel electrode and is significantly influenced by ligation geometry and solvation.[45,46] Therefore, it is logical to observe that the hydroxy-salen compounds adopt a square-planar geometry whereas the *k* value for the non-hydroxylated salen−Cu complex is more consistent with a tetrahedral distortion (Table 1). The square-planar anionic coordination environment inhibits axial interaction and favors the d^8 Cu^{III} oxidation state.[47]

An additional interesting issue of this work concerns the production of H$^{\bullet}$ radicals. As indicated in Figure 10, it is plausible that the hydroquinone−Cu^{III} complex evolves into a semiquinone−Cu^{III} complex with concomitant production of H$^{\bullet}$ radicals. The characterization of the DMPO−H$^{\bullet}$ adducts attests that this reaction occurs, at least under relatively high potential conditions (between 0 and 500 mV). The increase of the potential value facilitates the production of the Cu^{III} species and the formation of the semiquinone radical (at +0.566 V), but there is no direct evidence that the same reaction takes place under the conditions employed for the DNA cleavage experiments. The detection of H$^{\bullet}$ and $O_2^{\bullet -}$ radicals by spin trapping is consistent with the formation of a semiquinone radical when the hydroxyl groups are positioned in the *para* position (**3c**). In theory the semiquinone system cannot function with the hydroxyl in the *meta* position, and this is exactly what we observe. The hydroxyl groups in the *ortho* or *para* positions reinforce the σ donor effect of the oxygen atoms involved in the metal complexation. There is no doubt that the position of the OH is crucial in order to activate the copper complex.

In conclusion, the experimental data suggest that the hydroquinone system cooperates with the copper moiety to facilitate the formation of Cu^{III} species and free radicals responsible for DNA cleavage. We intend to use the original hydroquinone/semiquinone system described here with other metal−salen complexes, in particular with Fe−hydroxy-salens which efficiently mimick the activity of nucleases.

Experimental Section

Synthesis. The purity of all compounds was assessed by TLC, ^{1}H and ^{13}C NMR, and mass spectroscopy. TLC was carried out using silica gel 60F-254 (0.25 mm thick) precoated UV-sensitive plates. Spots were visualized by inspection under visible or UV light at 254 nm. Melting points were determined in a hot plate microscope and are uncorrected.

(43) Kitajima, N.; Moro-oka, Y. *Chem. Rev.* **1994**, *94*, 737.

(44) Bertini, I.; Luchinat, C.; Brown, R. D.; Koenig, S. H. *J. Am. Chem. Soc.* **1989**, *111*, 3532.

(45) Cole, A. P.; Root, D. E.; Mukherjee, P.; Solomon, E. I.; Stack, T. D.P. *Science* **1996**, *273*, 1848.

(46) Coleman, B.; Conrad, N. D.; Baum, M. W.; Jones, M. *J. Am. Chem. Soc.* **1979**, *101*, 7744.

(47) Hamilton, D. E.; Drago, R. S.; Telser, J. *J. Am. Chem. Soc.* **1984**, *106*, 5353.

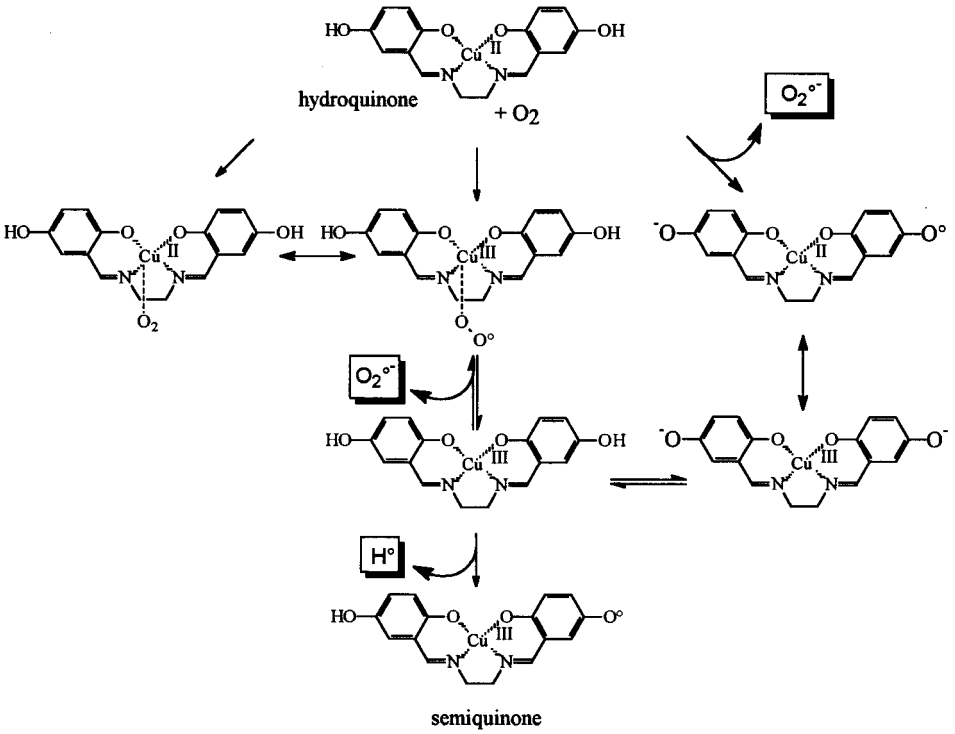

Figure 10. Proposed mechanism for the production of free radicals by compound **3c**. Reaction of the hydroquinone **3c** with oxygen leads to the oxidation of Cu^{II} to Cu^{III}. The transient Cu^{III}−superoxo complex then dissociates, producing superoxide anions and the Cu^{III}−hydroquinone complex, which in turn can provide hydrogen radicals and the Cu^{II}−semiquinone complex. The free radicals (detected by spin trapping) would be reponsible for DNA cleavage.

^1H and ^{13}C NMR spectra were recorded on a Bruker AC300. Chemical schifts (δ) are referenced to internal solvent and reported relative to $SiMe_4$. IR spectra were obtained using KBr pellets, and only the principal sharp peaks are given. MALDI (mass-assisted laser desorption ionization) mass spectra were determined on a Finigan MAT Vision 2000 (Bremen). The matrix used was dihydroxybenzoic acid/water.

Hydroxy-salen−copper complexes **3a,b,c** were obtained using a conventional procedure for salen synthesis based on the condensation of hydroxysalicylaldehyde with ethylenediamine (Scheme 1).[20] The copper complex formation was achieved with **2a,b,c** in the presence of cuprous acetate monohydrate. The synthesis of the non-hydroxylated analogue **3d** has been reported.[20]

***N,N′*-Bis(hydroxysalicylidene)ethylenediamine (2a,b,c)**. A solution of 1.88 g (13.61 mmol) of dihydroxybenzaldehyde (**1a,b,c**) (Sigma Chemical Co., France) and 0.40 g (6.66 mmol) of ethylenediamine in toluene (150 mL) was refluxed under vigorous stirring with a Dean−Stark apparatus for 3 h. The resulting solution was kept at room temperature for 1 h prior to being filtered and washed successively with ethanol (2 × 10 mL) and ethyl ether (2 × 10 mL) to afford compounds **2a,b,c**.

Data for compound **2a** (1.96 g; 98%): orange solid; mp > 230 °C; IR (KBr, cm^{-1}) ν 3400, 1540, 1460, 1380, 1360, 1280, 1240, 1200, 1020, 900, 860, 790, 740; MS (MALDI$^+$) *m/z* 301.4 $(M + H)^+$, 323.5 $(M + Na)^+$; R_f (CH_2Cl_2/MeOH, 8:2) 0.78; ^1H NMR (DMSO-d_6) δ 3.92 (s, 4H), 6.64 (t, $J = 7.6-7.8$ Hz, 2H), 6.83 (m, 4H), 8.54 (s, 2H), 12.8 (s, 2H); ^{13}C NMR (DMSO-d_6) δ 58.04 (CH_2), 117,69 (CH), 117,76 (CH), 118.2 (Cq), 121.86 (CH), 145,85 (Cq), 151,10 (Cq), 167.19 (CH).

Data for compound **2b** (1.94 g; 97%): orange solid; mp > 230 °C; IR (KBr, cm^{-1}) ν 2800, 1640, 1580, 1500, 1480, 1360, 1280, 1240, 1210, 1160, 1120, 1000, 980, 840, 800, 610; MS (MALDI$^+$) *m/z* 301.4 $(M + H)^+$; R_f (CH_2Cl_2/MeOH, 8:2) 0.56; ^1H NMR (DMSO-d_6) δ 3.76 (s, 4H), 6.14 (d, $J = 2.2$ Hz, 2H), 6.24 (dd, $J = 2.2$, 8.3 Hz, 2H), 7.15 (d, $J = 8.3$ Hz, 2H), 8.35 (s, 2H), 12.6 (s, 2H); ^{13}C NMR (DMSO-d_6) δ 57.66 (CH_2), 102.58 (CH), 106.96 (CH), 111.12 (Cq), 133.39 (CH), 161.97 (Cq), 164.63 (Cq), 165.8 (CH).

Data for compound **2c** (1.93 g; 97%): orange solid; mp > 230 °C; IR (KBr, cm^{-1}) ν 3320, 1640, 1600, 1510, 1450, 1410, 1310, 1260, 1220, 1180, 1040, 970, 860, 840, 800, 680; MS (MALDI$^+$) *m/z* 301.4 $(M + H)^+$, 323.5 $(M + Na)^+$, 339.4 $(M + K)^+$; R_f (CH_2Cl_2/MeOH, 8:2) 0.90; ^1H NMR (DMSO-d_6) δ 3.86 (s, 4H), 6.64−6.79 (m, 6H), 8.46 (s, 2H), 12.51 (s, 2H); ^{13}C NMR (DMSO-d_6) δ 59.03 (CH_2), 116.47 (CH), 116.85 (CH), 118.5 (Cq), 119.88 (CH), 149.27 (Cq), 152.99 (Cq), 166.33 (CH).

[*N,N′*-Bis(hydroxysalicylidene)ethylenediamine]copper (3a,b,c). A solution of **2a,b,c** (0.250 g, 0.83 mmol) in dry ethanol (20 mL) and cuprous acetate monohydrate (0.170 g, 0.83 mmol) in water (2 mL) was refluxed under vigorous stirring for 2 h. After this time, the resulting solution was kept at room temperature, filtered, and then washed successively with water, methanol, and ethylic ether (3 × 10 mL) to afford compounds **3a,b,c**. NMR spectra of complexes **3a,b,c** exhibit a broadened line in the aromatic region due to the paramagnetism of Cu^{II} (this well-known phenomenon leads to poor resolution of the spectra).

Data for compound **3a** (0.211 g; 70%): brown solid; mp > 230 °C; IR (KBr, cm^{-1}) ν 3400, 1620, 1550, 1450, 1400, 1310, 1280, 1220, 870, 740, 620; MS (MALDI$^+$) *m/z* 362.3 $(M + H)^+$, 384.4 $(M + Na)^+$, 301.4 $(M + 3H - Cu)^+$; R_f (CH_2Cl_2/MeOH, 80:20) 0.74.

Data for compound **3b** (0.268 g; 89%): purple solid; mp > 230 °C; IR (KBr, cm^{-1}) ν 3400, 1620, 1540, 1440, 1340, 1220, 1180, 1130, 990, 850, 800, 650; MS (MALDI$^+$) *m/z* 362.1 $(M + H)^+$, 384.2 $(M + Na)^+$, 400.2 $(M + K)^+$, 301.2 $(M + 3H - Cu)^+$; R_f (CH_2Cl_2/MeOH, 80:20) 0.74.

Dat for compound **3c** (0.259 g; 86%): black solid; mp > 230 °C; IR (KBr, cm^{-1}) ν 3200, 1630, 1540, 1460, 1400, 1370, 1320, 1220, 1150, 1080, 970, 860, 840, 800; MS (MALDI$^+$) *m/z* 361.5 $(M + H)^+$, 301.3 $(M + 3H - Cu)^+$; R_f (CH_2Cl_2/MeOH, 80:20) 0.52.

Voltammetry. Cyclic voltammetry measurements were performed with a SOLEA TACUSSEL PJT 120 potentiostat equipped with a programmable interface SOLEA TACUSSEL IMT1. Working and auxiliary electrodes were a platinum CTV 101T and a platinum wire, respectively. The standard calomel reference electrode was separated from the bulk of the solution by a KCl saturated solution with a glass frit. A scan rate of 50 mV s^{-1} gave the best results.

The electrolyte support salt was tetraethylammonium perchlorate (0.1 N), and prior to use, all solutions were made in DMSO freshly distilled with calcium hydride (CaH_2) under an inert atmosphere. The complex

mixtures (1 mM) were deoxygenated by means of a stream of dry nitrogen. A nitrogen stream was maintained above the solutions during the electrochemical measurements.

Electron Spin Resonance. X-band ESR spectra were obtained with both a Bruker ESC 106 and a Varian E-9 operating at 100 kHz modulation frequency at room temperature (20 °C) or at liquid nitrogen temperature (77 K). The *g* factor measurements were related to the "strong pitch", $g = 2.0028$. For spin trapping experiments, DMPO (5,5′-dimethylpyrroline *N*-oxide, Sigma Chemical Co.) was added to the mixtures.

ESR measurements coupled to electrochemistry were performed in a TM cavity mode with 0.1 cm flat quartz cell. The anodic and cathodic platinum electrodes were connected to a SOLEA TACUSSEL PJT 120 potentiostat to monitor the imposed voltage. Calomel electrodes were used as references.

Simulations of isotropic nitrogen superhyperfine interactions in the complex were performed with the Bruker WINSIMFONIA software.

DNA Cleavage. Each reaction mixture contained 9 μL of supercoiled pUC12 DNA (0.5 μg in a Tris−HCl, 10 mM NaCl buffer at pH 7.0) and 1 μL of the test compound at the desired concentration in DMSO. After 1 h of incubation at 37 °C, 4 μL of loading buffer (0.25% bromophenol blue, 0.25% xylene cyanol, 30% glycerol in H_2O) was added to each tube and the solution was loaded onto a 1% agarose gel. The electrophoresis was carried out for about 2 h at 100 V in TBE buffer (89 mM, Tris−borate, pH 8.3, 1 mM EDTA). Gels were stained with ethidium bromide (1 μg/mL) and then destained for 30 min in water prior to being photographed under UV light.

Acknowledgment. The authors thank Hélène Jary for her significant contribution to the synthesis of the complexes. This work was supported by grants (to C.B.) from the Association pour la Recherche sur le Cancer and (to J-L.B. and J-P.C.) from the CNRS.

Supporting Information Available: Figures showing the simulated spectra of DMPO−OOH, DMPO−CH_3, and DMPO−H and the experimental spectrum of the semiquinone species (PDF). This material is available free of charge via the Internet at http://pubs.acs.org.

JA982221Z